

1996

Optimizing the Design of a Thermoacoustic Refrigerator

B. L. Minner
Purdue University

J. E. Braun
Purdue University

L. Mongeau
Purdue University

Follow this and additional works at: <http://docs.lib.purdue.edu/iracc>

Minner, B. L.; Braun, J. E.; and Mongeau, L., "Optimizing the Design of a Thermoacoustic Refrigerator" (1996). *International Refrigeration and Air Conditioning Conference*. Paper 343.
<http://docs.lib.purdue.edu/iracc/343>

This document has been made available through Purdue e-Pubs, a service of the Purdue University Libraries. Please contact epubs@purdue.edu for additional information.

Complete proceedings may be acquired in print and on CD-ROM directly from the Ray W. Herrick Laboratories at <https://engineering.purdue.edu/Herrick/Events/orderlit.html>

OPTIMIZING THE DESIGN OF A THERMOACOUSTIC REFRIGERATOR

B.L. Minner, J.E. Braun, and L. Mongeau
Ray W. Herrick Laboratories
Purdue University
West Lafayette, IN 47907

INTRODUCTION

Unconventional cooling technologies are currently being explored, or revisited, in response to environmental concerns related to many refrigerants widely used in vapor compression cycles. Thermoacoustic cooling devices show promise as alternative cycles because they: 1) utilize environmentally benign working fluids, 2) use energy in the form of either electricity or heat, such as from a natural gas burner, 3) can achieve low temperatures with simple designs, 4) have continuous capacity control, 5) have no sliding seals and do not require the use of lubricants, 6) could potentially be made quiet (Garfinkel, 1994) and 7) require small compression ratios, allowing the use of electro-acoustic transducers such as loudspeakers in place of mechanical compressors. Ultimately, the simplicity of thermoacoustic devices could lead to both low manufacturing and low maintenance costs.

A thermoacoustic heat pump, which uses acoustic power to provide a net cooling effect, comprises four basic elements, as shown in Figure 1. The elements are: 1) a "stack" made of porous material, parallel plates, or sheets of thin solid material rolled up into a spiral; 2) hot and cold heat exchangers consisting of finned tubes, parallel plates, screens, or metallic wool; 3) a rigid and sealed tube termination which often incorporates a Helmholtz resonator in order to shorten the device and minimize extraneous losses; and 4) an acoustic energy source, which is usually an electro-acoustic transducer. The working fluid is usually a mixture of several perfect gases, such as helium and xenon. The driver operates at the resonant frequency of the system to produce relatively large pressure fluctuations that alternately compress and expand the working fluid and cause the fluid to oscillate back and forth within the stack and heat exchangers. For the system of Figure 1, the largest pressure fluctuations (pressure anti-node) occur at the driver, while the largest velocity fluctuations occur near the entrance to the Helmholtz resonator.

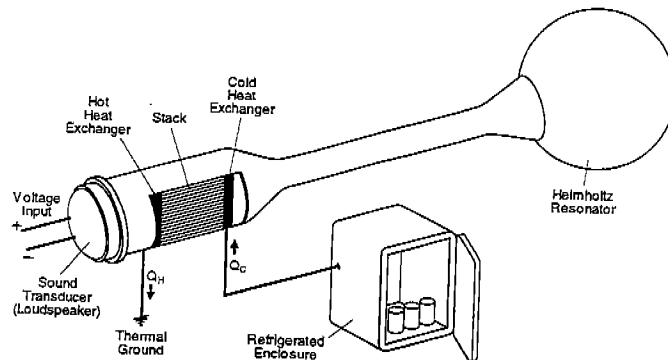


Figure 1. Thermoacoustic Refrigerator Concept

The principles of operation within the stack are illustrated in Figure 2. Acoustically driven fluid particles, located close to surfaces within the stack, undergo a cycle similar to the reversed Brayton cycle. They pump heat from the cold heat exchanger against an adverse temperature gradient to the hot heat exchanger. The displacement and compression processes in ideal standing waves are in phase, such that between states 1 and 2, fluid particles are compressed and simultaneously displaced. At state 2, the particle velocity changes direction, such that the particle "dwells" near one location for a portion of a cycle, giving time for a thermal exchange between the compressed fluid and the solid to take place. In the heat exchange process between states 2 and 3, the fluid cools to a lower temperature. Between states 3 and 4, the fluid is expanded and displaced. Because of the heat transfer that occurred between states 2 and 3, the fluid is now cooler than the surface and is warmed in order to return to state 1. The net effect of the cycle is that the fluid has "moved" energy from one portion of the stack to another, storing it in the solid for removal by another particle during the expansion phase of its cycle. The net energy transfer occurs in the direction that the fluid

moves when the compression process occurs (towards the pressure anti-node of the standing wave). The resulting gradient in the mean temperatures of the fluid and the solid causes adverse heat conduction, effectively reducing the amount of heat pumped by the fluid.

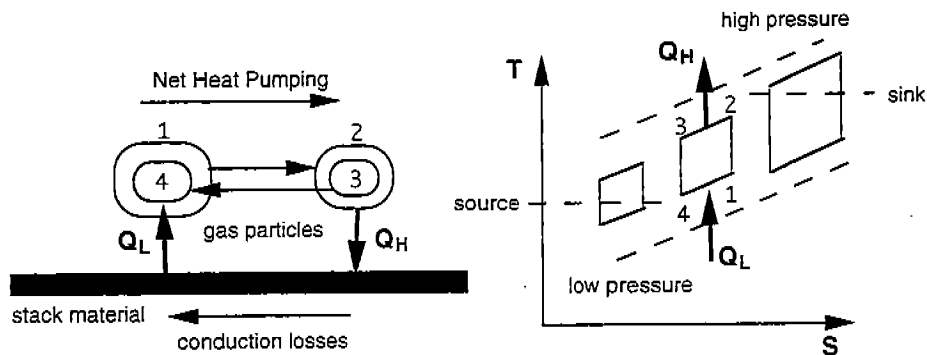


Figure 2. Thermoacoustic Cycle Representation

The stack is not necessary for an operational thermoacoustic cooler, but it does serve a useful function. Without a stack, it is possible to displace the fluid between hot and cold heat exchangers that are separated by a finite gap. In this case, fluid that contacted both heat exchangers during an acoustic oscillation would undergo a cycle similar to a single-stage Brayton cycle operating between high and low pressures dictated by the temperature requirements for the hot and cold heat exchangers. The performance of this "stackless" device may be no better than a standard reverse Brayton cycle that utilizes separate components for the compressor, turbine, and heat exchangers (although it is much simpler and therefore probably less expensive and more reliable). The addition of the stack allows "cascading" as depicted in the T-s diagram of Figure 2. An element of fluid that is only displaced part of the way between the heat exchangers only undergoes a portion of the temperature rise required between the low and high temperature heat exchangers and therefore requires a much smaller pressure rise. The smaller fluid compression ratios result in smaller irreversibilities in both the compression and expansion portions of the cycle. The stack is an extremely simple and inexpensive means of achieving cascading. Cascading for a standard Brayton cycle would require multiple compressors, turbines, and heat exchangers and would be cost prohibitive. The stack does impose penalties on system performance in the form of additional viscous losses and conduction losses.

The early history of thermoacoustics was well documented in the comprehensive review article by Swift (1988). The development of practical applications for thermoacoustic cooling was initiated in the United States in the early eighties by Wheatley et al. (1983). Since that time, several prototypes have been built (Garrett, 1993). Although the efficiency of prototypes is improving, it is at 20-30% of Carnot efficiency (Swift, 1995), still below acceptable levels. However, previous prototype designs were based upon heuristic approaches and were not formally optimized.

This paper demonstrates the benefits of system optimization for the design of thermoacoustic refrigerator prototypes. A commercially available thermoacoustic system modeling software (Ward and Swift, 1993) was coupled to a direct search optimization and a detailed heat exchanger model. The criterion for optimization was overall efficiency for a specified cooling capacity and set of operating temperatures. The potential gains in performance from a systematic optimization are first illustrated in a case study whereby a device originally built and tested by Hofler (1986) was optimized. A thermoacoustic system for a domestic refrigeration application is then considered as a benchmark for the performance and size of thermoacoustic systems as compared with conventional vapor compression equipment.

DESIGN OPTIMIZATION

The goal of the optimization scheme was to determine designs that would maximize the coefficient of performance (cooling rate divided by the power input) for specified environmental temperatures and cooling capacities. Only geometrical and fluid parameters were optimized for devices similar in basic design to that depicted in Figure 1, although different configurations could readily be investigated.

The heat exchangers and stack were chosen to be parallel plates. Both a copper alloy ($k = 100 \text{ W/m-K}$) and perfect (infinite k) heat exchangers were considered. The use of perfect heat exchangers provides a benchmark for possible improvements. The stack should be made from a material with low thermal

conductivity and high specific heat. A low conductivity minimizes adverse heat conduction which occurs in a direction opposite to the heat pumping. A high specific heat reduces stack temperature fluctuations which reduce heat transfer rates between the stack and working fluid (see Figure 2). In this study, the stack was made of kapton ($k = 0.19 \text{ W/m-K}$, $c = 1.15 \text{ KJ/kg-K}$).

An ideal transducer mechanism with a 100% efficiency was considered. All of the electrical input was assumed to be converted into useful work imparted to the working fluid. This assumption is not unreasonable since acoustic drivers can be built with efficiencies near 90%. Both pure helium and a mixture of 50% of helium and xenon by mass were considered as working fluids in this study. The mean pressure of the fluid was a free variable in the optimization scheme. It is directly related to the amount of working fluid added to the system and affects fluid thermal and acoustic properties.

The design optimization involved maximizing the cost function

$$J = COP(\mathbf{d}, \mathbf{x}) \quad (1)$$

with respect to a design vector \mathbf{d} and subject to a vector of external environmental conditions, \mathbf{x} , and subject to constraints that the thermoacoustic device must provide a specified cooling capacity, the system must be driven at the resonance frequency, and the design parameters must fall within reasonable bounds.

The design vector included the following parameters:

$$\mathbf{d}^T = \{d_1, d_2, d_3, d_{HR}, x_1, x_2, x_3, \Delta x_h, t_h, y_{o,h}, \Delta x_c, t_c, y_{o,c}, \Delta x_s, t_s, y_{o,s}, P_m\} \quad (2)$$

where d_1, d_2, d_3 , and d_{HR} are inner diameters of the thermoacoustic enclosure at the stack, cold duct, inlet to the Helmholtz resonator, and Helmholtz resonator, respectively; x_1, x_2 , and x_3 are the lengths of the hot duct (acoustic driver to hot heat exchanger), cold duct (cold heat exchanger to horn) and horn (prior to the helmholtz resonator) sections; $\Delta x, t$, and y_o are the lengths, plate thicknesses, and half-plate spacings associated with the hot heat exchanger, cold heat exchanger, and stack (subscripts h, c, and s refer to hot, cold, and stack); and P_m is the mean pressure of the fluid.

The external environmental conditions are:

$$\mathbf{x}^T = \{T_{ext,h}, T_{ext,c}\} \quad (3)$$

where $T_{ext,h}$ and $T_{ext,c}$ are temperatures at the exterior walls of the hot and cold heat exchangers, respectively. It was assumed that these exterior walls were maintained at specified temperatures through the use of secondary fluids. The secondary heat exchanger loop was not modeled in this study.

Given a guess of the design vector, the known external environmental conditions, and the specified cooling capacity, a model of the thermoacoustic device described in the next section was used to determine the COP and the acoustic driver operating parameters necessary to achieve the desired operating conditions. The driver operating frequency, f , the volume velocity, U_o , and the pressure amplitude, p_o , were all adjusted to force the system into resonance and provide the required cooling capacity. Updates of the design vector were generated using the Simplex method (Nelder & Mead, 1965), which relies on direct search of the parameter space and does not require the evaluation of partial derivatives or gradients. This method is robust and easily handles constraints. However, it can be computationally inefficient and it does not guarantee that a global minimum will be obtained. Parameters such as material thickness and heat exchanger fin lengths were constrained based upon practical limitations. Additional constraints considered in some case studies included limits on mean pressure, drive ratio, and stack diameter. A complete description of the optimization and modeling methods and constraints is provided by Minner (1996).

THEORETICAL MODEL

A commercially available software, Design Environment for Low Amplitude ThermoAcoustic Engines (DELTAE; Ward and Swift, 1993), was used to determine the power input for a given design vector, imposed operating (boundary) conditions, and target capacity. A detailed discussion of the modeling assumptions and equations is given by Swift (1988). Nonlinear effects such as acoustic streaming, boundary layer turbulence, and wave steepening are neglected in DELTAE. These phenomena are normally associated with high drive

ratios (ratio of maximum system pressure amplitude to mean pressure, p_o/P_m). Nonlinear effects would cause the model to over predict performance for high drive ratios. Good comparisons between model and experimental results have been reported for drive ratios near 5%, while poorer results have been obtained for drive ratios approaching 10% (Swift, 1992). In this optimization study, drive ratios were constrained to be less than 3% for the Hofler device and 9% for the refrigerator application.

DELTAE does not properly consider the effects of abrupt geometrical changes, since the effects of boundary layer separation and reattachment downstream are neglected. Therefore, the benefits of gradual transitions between segments associated with reduced viscous losses are not considered. Two-dimensional computational (CFD) methods would be needed to model these complex phenomena.

DELTAE also does not consider heat conduction in the heat exchanger metal. In order to consider optimization of the heat exchangers, a simple heat transfer model was developed in this study for a parallel plate configuration. Each plate was considered to be a fin interacting with a working fluid at a constant and uniform temperature equal to the mean fluid temperature within the heat exchanger. Each fin was assumed to have a temperature distribution between the outer wall and an adiabatic center line that did not vary with time. The heat transfer rate between the fluid and the outside wall was estimated as

$$\dot{Q} = \sum_{i=1}^{N_f} \phi_{f,i} h_o A_{f,i} (T_m - T_{ext}) \quad (4)$$

where N_f is the number fins (parallel plates) within the heat exchanger, $\phi_{f,i}$ is the fin efficiency for the i^{th} fin, h_o is the overall heat transfer coefficient between the surface and the fluid, $A_{f,i}$ is the surface area in contact with the i^{th} fin, T_m is the mean fluid temperature, and T_{ext} is the exterior wall temperature for either the hot or cold heat exchanger. The fin efficiency is the ratio of the actual heat transfer rate to the heat transfer that would occur if the fin were at the wall temperature. Relationships for straight fins (Incropera and Dewitt, 1990) were used to evaluate the fin efficiencies for each plate between the wall and the adiabatic centerline. The perfect heat exchanger had fin efficiencies of unity. The average heat transfer coefficient was estimated assuming conduction through the fluid within a laminar boundary layer, such that

$$h_o = \frac{k_f}{\Delta y_k} \quad (5)$$

where k_f is the fluid thermal conductivity and Δy_k is the average thickness of the boundary layer during an acoustic oscillation. The boundary layer thickness was estimated as the minimum of half the plate spacing (y_o) and the thermal penetration depth. The thermal penetration depth is defined as the distance through which heat can diffuse in one acoustic cycle (Swift, 1988) and is determined as

$$\delta_t = \sqrt{\frac{\alpha_f}{\pi f}} \quad (6)$$

where α_f is fluid thermal diffusivity and f is acoustic frequency. The use of thermal penetration depth as a conduction thickness is conservative since turbulence effects would reduce the boundary layer thickness.

MODEL VALIDATION

The model was validated by comparing performance predictions with experimental results reported by Hofler (1986) for the configuration shown in Figure 1. A drive ratio (p_o/P_m) of 0.03 was used, consistent with Hofler's tests. The experimental procedure involved holding the input power of the driver constant, while the thermal load at the cold heat exchanger was varied and the temperatures of the heat exchanger surfaces were measured as a function of thermal load. Figure 3 presents simulated and experimental results for COP relative to Carnot and temperature ratio T_c/T_h as a function of total heat flux, Q_{tot} . The theoretical model over predicts performance by 13.7% on average. It is believed that thermal leaks and other "nuisance" loads may be responsible for the discrepancies at lower capacities [Hofler, 1986, p. 114]. The heat exchanger model

predicted the temperature difference between the center and circumference of the heat exchanger to within 0.1 C of the measured value of 4.1 C at a heat rejection rate of 18W.

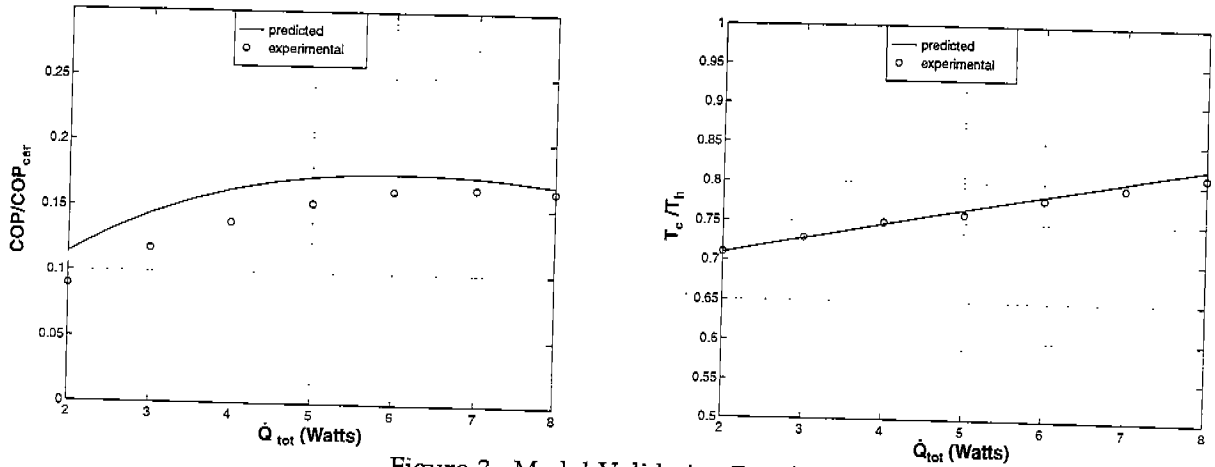


Figure 3. Model Validation Results

OPTIMIZED HOFLER DEVICE

The Hofler prototype was optimized for a 6 Watt capacity and cold and hot side wall temperatures of 230 and 300 K for four different combinations of working fluid and mean pressure constraints. A comparison of the performance and required drive ratio, volume velocity, and operating frequency is given in Table 1 for each of the optimized cases and the original Hofler design. The coefficient of performance (COP) is normalized by the Carnot COP, which is 3.29 for reservoirs at temperatures of 230 and 300K.

Table 1. Comparisons of Optimized and Hofler Devices

Case	Helium Fraction	P_m (bars)	COP/COP_c	P_o/P_m	U_o (cm ³ /s)	f (hz)
Hofler	1.0	= 10	0.17	0.035	835	505
1	1.0	< 10	0.33	0.029	390	232
2	1.0	< 50	0.36	0.018	117	143
3	0.5	< 10	0.43	0.030	298	101
4	0.5	< 50	0.50	0.028	64	64

Case 1, for which only geometrical parameters were varied, illustrates a 100% improvement over the Hofler design in performance. Case 2, for which the constraint on P_m was relaxed, resulted in performance that is approximately 115% better than that of the Hofler case. Case 3 displays a 162% improvement in performance, subject to a 10 bar mean pressure constraint and a 50% helium-xenon mixture. Case 4 achieves a 205% increase in performance, subject to a 50 bar mean pressure constraint and a 50% helium-xenon mixture.

Figure 4 depicts the geometry associated with the five cases. The stacks of the optimized designs are shorter and larger in diameter, and are positioned closer to the driver, than are those in the Hofler prototype. In addition, ratios of stack diameter to cold duct diameter are higher, the spacing of the stack plates is comparable but reduced, the heat exchangers are shorter as a fraction of particle displacement, and their spacing relative to the thermal penetration depth is generally greater. The cold duct sections, or those duct segments between the cold heat exchanger and the Helmholtz resonator, are longer, as is the wavelength of sound, except for case 3. Overall, the optimized systems occupy more volume.

The case 1 improvements are solely due to geometrical changes that result in lower system losses. This case demonstrates the importance of design optimization for thermoacoustic systems. The optimized design results from tradeoffs between thermal and viscous losses in different parts of the system. Thermal losses are due to inefficient heat exchangers, parasitic conduction within the stack and fluid, and unwanted heat pumping that occurs at heat exchanger and duct surfaces. The shorter stack in the optimized case 1 (as compared with the Hofler prototype) results in smaller viscous losses, but greater conduction losses. The size of the heat exchangers increase to give smaller temperature differences between surfaces and the fluid at the

expense of additional viscous losses. The optimal placement of the stack results from a tradeoff between pressure and velocity fluctuations. The "local" heat flux in the stack depends upon the rate at which work is performed on the fluid which is directly related to the product of the fluid pressure and velocity amplitudes. Furthermore, viscous are directly related to the fluid velocities. Positioning the stack closer to the pressure anti-node (velocity node) reduces volume velocities of the fluid, while increasing the compression ratio.

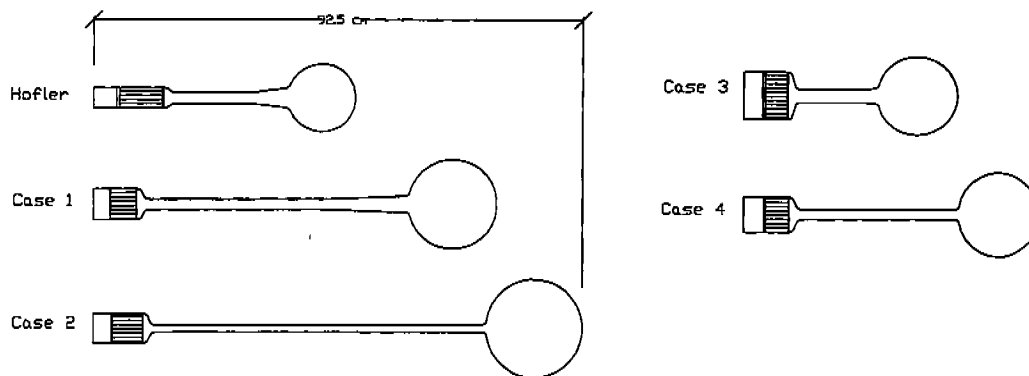


Figure 4. Comparison of Hofler and Optimized Geometries

A comparison of results for cases 1 and 2 demonstrates the effect of mean pressure on the optimized design and performance. In both cases, the optimization gave mean pressures at the upper limit (10 and 50 bar). The performance improves with increasing mean pressure because of increasing fluid density. A higher density fluid requires a lower drive ratio to achieve a given fluid pressure amplitude and a lower driver volume velocity to realize a specific mass fluctuation. Both effects reduce the power required to achieve a particular cooling capacity. The results of Table 1 show that the capacity was achieved with a lower drive ratio and volume velocity for the higher mean pressure. In comparing the geometries for cases 1 and 2, it is apparent that lower fluid velocities have resulted in longer and narrower sections because viscous losses are lower.

The effect of the fluid mixture can be seen by comparing the results of cases 1 and 3. The improvement in performance for the mixture of helium and xenon results from a lower Prandtl number. The Prandtl numbers for the helium and helium-xenon working fluids are approximately 0.68 and 0.20, respectively. The Prandtl number determines the ratio of viscous to thermal boundary layer thickness, so a lower Prandtl number results in lower viscous losses for the same thermal diffusion. This effect is offset, somewhat, by a reduction in sound speed and thermal conductivity with increasing concentrations of xenon. In this study, a 50/50 mixture of xenon and helium was found to be nearly optimal. The helium-xenon mixture also results in a shorter device, a lower operating frequency, and a higher drive ratio. The stack is shorter for case 3 than 1 because of the lower conductivity of the helium-xenon mixture as compared with pure helium.

The comparison between cases 3 and 4 shows similar trends as for cases 1 and 2. However, for the helium-xenon mixture, the performance is more sensitive to mean pressure.

AN OPTIMIZED REFRIGERATOR

A thermoacoustic device based upon the Hofler configuration with a 50/50 mixture of helium-xenon was optimized to provide the best COP while pumping 200 watts of heat from a source at 260 K to a sink at 310 K. The operating conditions and cooling capacity are typical of a home refrigerator. In addition to geometry constraints, the mean pressure and drive ratio were limited to 20 bars and 9%. Table 2 shows COP and drive ratio, volume velocity, and operating frequency results for copper heat exchangers and perfectly conducting heat exchangers both without a diameter constraint and with a diameter constraint of 5 inches (12.7 cm).

The performance of the device with copper heat exchangers and constrained diameter is the lowest. However, its COP is comparable to a conventional refrigeration system for these operating conditions. The use of a highly conductive material has a dramatic impact on performance. Although perfect heat exchange is not possible, these results do demonstrate the importance of utilizing efficient heat exchangers. Conduction heat exchangers are particularly poor at higher cooling capacities, because of the need for larger diameters. The copper heat exchangers for the refrigerator have overall fin efficiencies of less than 10% for the diameter constrained case. In contrast, the fin efficiencies for the lower capacity case 3 described in the previous section were about 40%. The use of finned tubed heat exchanger is a practical approach to achieving

good performance at higher capacities. For this application, the secondary fluid could be water for the hot heat exchanger and a mixture of water and glycol for the cold heat exchanger. Alternatively, a phase fluid could be used as a secondary fluid.

Table 2. Comparison of Optimized Refrigerator Results

HX Type	Diameter Constraint	COP	P_o/P_m	U_o (cm ³ /s)	f (hz)
copper	5 inches	1.7	9.0	1358	62
copper	none	2.0	8.0	1261	41
perfect conductor	5 inches	2.6	9.0	875	67
perfect conductor	none	3.0	7.3	947	57

Table 2 also illustrates that freeing up the diameter constraint has a significant impact on performance. The optimal unconstrained diameter was found to be about 7.8 inches (19.7 cm) for the copper heat exchangers and 8.8 inches (22.4 cm) for the perfect exchangers. For large capacities, it may be necessary to either constrain the diameter or utilize multiple thermoacoustic devices arranged in parallel.

The drive ratios of the optimized devices are at the upper limit for the diameter constrained cases and less than the limit for the unconstrained diameters. In order to maintain cooling capacity when a diameter constraint is imposed, the drive ratio and/or volume velocity must increase. Higher volume velocities lead to greater viscous losses for a given design. Higher drive ratios require longer stacks in order to balance the temperature requirements of the heat exchangers and therefore also lead to greater viscous dissipation. In the absence of a diameter constraint, the lower drive ratio and volume velocity requirements lead to lower viscous losses and better performance.

Figure 5 depicts the geometries of the constrained diameter thermoacoustic devices. These devices are shorter than the low capacity coolers of Figure 4, even though the cooling requirement is about 30 times greater. However, the cross-sectional area and total volume are significantly greater. The power density of both optimized devices is about 1 ton/ft³, which is about 5 times greater than those of low capacity devices. The copper heat exchangers require significantly more surface area for heat transfer than the low capacity cases, resulting in greater viscous dissipation and lower overall efficiency.

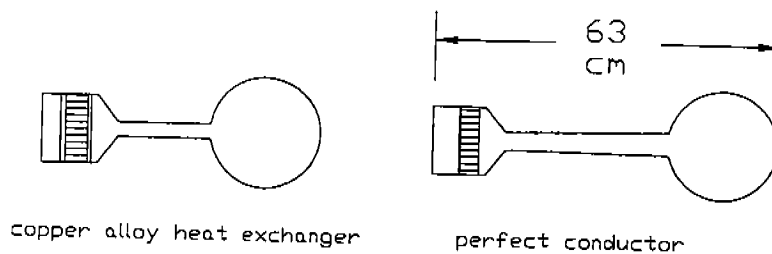


Figure 5. Comparison of Optimized Refrigerator Geometries (Constrained Diameters)

The cooling capacity of a thermoacoustic device is controlled by changing the amplitude of fluctuation in the driver mechanism which changes both the drive ratio and volume velocity. Figure 6 shows the effects of cooling capacity and cold heat exchanger supply temperature on COP and drive ratio for the optimized device with copper heat exchangers and constrained diameter. The COP is a weak function of capacity at a given cold wall temperature, but is more sensitive to operating temperature. The good part-load performance of thermoacoustics could represent a major advantage when compared to vapor compression technology. The drive ratio requirement is a strong function of capacity, since it is directly related to the capacity control.

CONCLUSIONS

A tool was developed for optimization of thermoacoustic devices that attempts to maximize efficiency. The modeling tool, which is based upon acoustic boundary layer theory and conventional heat exchanger analysis, was validated using documented experimental results for a well known prototype (Hofler, 1986). The optimization tool was then applied to this prototype in order to demonstrate the benefits of optimal

design. The improvement in COP achieved by the optimized devices ranged from 100% to 200%, depending upon the working fluid and mean pressure limits utilized. In general, mixtures with lower Prandtl numbers and higher mean pressures provided better performance.

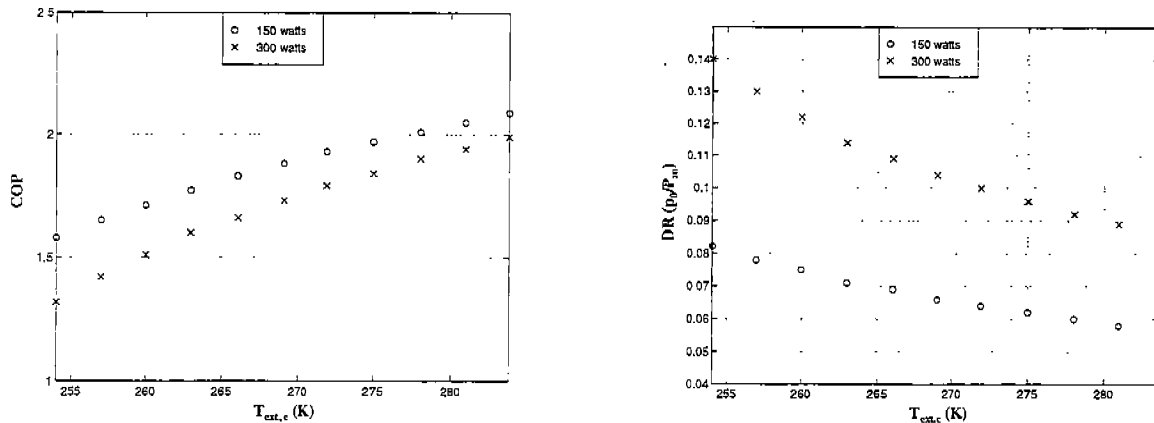


Figure 6. Off-Design Thermoacoustic Performance (Copper Heat Exchangers, Constrained Diameter)

Devices with a similar configuration were optimized for a home refrigerator application. Using conduction heat exchangers with copper, the predicted COP's were 1.7 with a 5 inch diameter constraint and 2.0 for an unconstrained diameter (7.8 inches). Although this performance is comparable to that of vapor compression refrigeration equipment, the conduction heat exchangers were found to be a major "bottleneck" to better performance. In order to demonstrate the importance of heat exchanger performance, the copper was replaced with a perfect conducting material and the COP improved to 2.6 and 3.0 for the constrained and unconstrained diameters, respectively. It is expected that a finned tube heat exchanger with a secondary fluid would result in performance between those of the copper and perfect conducting heat exchangers. Additional improvements are expected with improved stack and resonator designs.

Although the performance predictions are encouraging, especially given the many practical advantages of thermoacoustics (e.g., environmental, simplicity), there is need for further validation of the modeling tools and validation of the results of this study. The analysis did not include inefficiencies associated with the electroacoustic transducer. Although 90% efficient drivers are possible, the costs associated with these devices may be prohibitive. In addition, the effects of unmodeled non-linearities and flow separations at abrupt transitions may be significant for the optimized geometries. These negative effects on performance are countered, somewhat, by conservative assumptions regarding heat transfer within the heat exchangers. The heat transfer calculations assumed conduction across a laminar boundary layer. In reality, there will be turbulence that will increase the heat transfer coefficient between the fins and the primary working fluid.

REFERENCES

- Hofler, T.J. 1986. "Thermoacoustic Refrigerator Design and Performance," PhD Dissertation, Physics Department, University of California, San Diego, CA.
- Garrett, S.L.; Hofler, T.J.; & Perkins, D.K. 1993. "Thermoacoustic Refrigeration," Greenpeace Ozone-Safe Cooling Conference, October 1993, Washington, D.C.
- Incropera, F.P. & Dewitt, D.P. 1990 Fundamentals of Heat and Mass Transfer, 3rd Ed., Wiley & Sons, N.Y.
- Minner, B.L., 1996. "Optimization of Thermoacoustic Systems for Cooling Applications," M.S. Thesis, School of Mechanical Engineering, Purdue University, W. Lafayette, IN.
- Nelder, J.A. & Mead, R. 1965. *Computer Journal*, vol. 7, pp. 308-313.
- Swift, G.W. 1988. "Thermoacoustic Engines," *J. Acoust. Soc. Am.*, 84, pp. 1145-1180.
- Swift, G.W. 1992. "Analysis and Performance of Large Thermoacoustic Engine," *J. Acoust. Soc. Am.*, 92, pp. 1151-1163.
- Swift, G.W. 1995. "Thermoacoustic Engines and Refrigerators," *Physics Today*, July, pp. 22-28.
- Ward, W.C. & Swift, G.W. 1993. *Design Environment for Low-Amplitude Thermoacoustic Engines*, Tutorial and User's Guide. Los Alamos National Laboratory, N.M.
- Wheatley, J.C.; Hofler, T.J.; Swift, G.W.; & Miglior, A. 1983. "An Intrinsically Irreversible Heat Engine," *J. Acoust. Soc. Am.*, 74, p. 153.